

## THE PRIMARY ORBIT AND THE ABSORPTION LINES OF HDE 226868 (CYGNUS X-1)

Z. NINKOV,<sup>1,2</sup> G. A. H. WALKER,<sup>1,2</sup> AND S. YANG<sup>2</sup>

Department of Geophysics and Astronomy, University of British Columbia

Received 1986 July 3; accepted 1987 February 12

## ABSTRACT

From Reticon spectra of  $\sim 1 \text{ \AA}$  resolution taken between 1980 and 1984, the radial velocity curve of HDE 226868 is found to be characteristic of a single-line spectroscopic binary with  $K = 75.0 \pm 1.0 \text{ km s}^{-1}$  and  $e = 0.0$ . Combining historical velocities from the literature with our own data and applying a period-folding analysis, a period of  $5.59964 \pm 0.00001$  days is found. These values agree well with those published by Gies and Bolton in 1982.  $v \sin i$  is estimated to be  $94.3 \pm 5 \text{ km s}^{-1}$  from CFHT Reticon spectra taken at  $0.1 \text{ \AA}$  resolution. Assuming that the rotation of the primary is synchronized to the orbital revolution of the secondary gives a primary to secondary mass ratio between 1.5 and 2.3.

An absolute magnitude of  $-6.5 \pm 0.2$  is derived from the equivalent width of  $H\gamma$  ( $1.5 \pm 0.1 \text{ \AA}$ ) and the 1985 calibration of Walker and Millward which is consistent with the spectral classification of O9.7 Iab. Assuming  $20 M_{\odot}$  as a reasonable estimate for the mass of the primary implies a mass of  $10 \pm 1 M_{\odot}$  for the secondary. The equivalent width of  $H\gamma$  and  $H\beta$  are 20% larger at zero phase (X-ray minimum) of the 294 day X-ray period. A variation in the outflow rate from the primary could produce variations in both the Balmer-line equivalent widths and the X-ray flux.

*Subject headings:* stars: individual (HDE 226868) — X-rays: binaries

## I. INTRODUCTION

Cygnus X-1 was one of the first X-ray sources detected (Bowyer *et al.* 1965), and it seems well established that it consists of an O star (HDE 226868) with a compact companion which is the source of the X-ray flux (Bolton 1972; Gies and Bolton 1982, 1986). Apart from a steady X-ray flux, Cygnus X-1 sporadically moves into an X-ray high state where its luminosity ( $< 10 \text{ keV}$ ) increases by  $\leq 10$  (Liang and Nolan 1984). Recently, Priedhorsky, Terrell, and Holt (1983) have identified in addition a small, regular X-ray variation ( $\sim 25\%$ ) with a  $294 \pm 4$  day period.

Early optical studies were mainly photographic with inherently low signal-to-noise ratio, and these left some questions unanswered. For example, is there any modulation in the spectroscopic data with the 294 day X-ray period or other periods proposed in the literature (e.g., 39/78 day period of Kemp, Herman, and Barbour 1978, the 4.5 year period of Wilson and Fox 1981).

The most interesting parameter for this system continues to be the mass of the secondary ( $M_x$ ). From the observed absence of X-ray eclipses, the value of the mass function, and the dereddened spectral flux of the primary, Paczyński (1974) and Bahcall (1980) derive a firm lower limit to  $M_x$  that is independent of the structure or of the evolutionary status of the system. The limit relies only on the distance to the system,  $d$ , and is given by

$$M_x \geq 3.4 M_{\odot} (d/2 \text{ kpc})^2.$$

The accuracy of the distance is thus a constraint on estimates of the minimum mass of the secondary using this technique. To date, distance has been estimated from the reddening-distance

<sup>1</sup> Visiting Astronomer, Canada-France-Hawaii Telescope operated by the National Research Council of Canada, the Centre National de la Recherche Scientifique of France, and the University of Hawaii.

<sup>2</sup> Visiting Astronomer, Dominion Astrophysical Observatory operated by the National Research Council of Canada.

correlation for nearby field stars (Margon, Bowyer, and Stone 1973; Bregman *et al.* 1973). Unfortunately in these studies, only three stars have distances  $> 2 \text{ kpc}$  while the majority are  $< 1.2 \text{ kpc}$ . Moreover, the accuracy of HD spectral classifications (i.e., spectroscopic distances) is questionable and the possibility of a patchy distribution of dust is ignored. Alternate distance determinations would be useful.

The 5.6 day orbital period of Cygnus X-1 is well established. There are theoretical models of the system (Kundt 1979) that, because of mass transfer between the system components, produce changes in the period. It was expected that observations over a wider range of epochs would improve the chance of detecting such period changes.

In an attempt to address these questions, we undertook a long-term monitoring program. We also tried to collect as many spectra as possible within single orbital periods (5.6 day) in order to look for cycle-to-cycle changes.

## II. OBSERVATIONS

The observations were taken with the 1.22 m (at  $40 \text{ \AA mm}^{-1}$  or  $0.6 \text{ \AA}$  per diode) and 1.83 m (at  $15 \text{ \AA mm}^{-1}$  or  $0.231 \text{ \AA}$  per diode) telescopes at the Dominion Astrophysical Observatory and with the Canada-France-Hawaii 3.6 m telescope (at  $2.4 \text{ \AA mm}^{-1}$  or  $0.036 \text{ \AA}$  per diode). The FWHM of the instrumental profile was about two or three diodes in all cases. The detector in all cases was a 30 mm long liquid nitrogen cooled EG&G RL1872F/30 Reticon. The system and data reduction procedures have been described in detail by Walker, Johnson, and Yang (1985). The dates and phases of the observations are listed in Table 1.

Figure 1 shows examples of typical spectra of 19 Cephei (*lower*) and HDE 226868 (*upper*). The blue spectra of Cygnus X-1 and 19 Cep were single exposures taken on 1982 August 7 with integration times of 7700 s and 900 s, respectively. The red spectra were taken on 1982 July 9 and have integration times of 7408 s and 1200 s, respectively. The signal-to-noise ratio is  $> 200$  on all exposures. Many of the lines in Figure 1

TABLE 1  
 MEAN RADIAL VELOCITIES FOR DIFFERENT EXCITATION ENERGY GROUPS ON  
 ALL NIGHTS THAT HDE 226868 WAS OBSERVED

BJD 2,440,000 +	Dispersion (Å per diode)	5.6 Day Binary Phase	294 Day X-Ray Phase	H (km s <sup>-1</sup> )	He I (km s <sup>-1</sup> )	He II (km s <sup>-1</sup> )	Metal (km s <sup>-1</sup> )
Centered at λ4686							
DAO 1.22 m:							
4513.770.....	0.600	0.282	0.322	61.7	64.9	75.1	87.1
4514.691.....	0.600	0.447	0.325	10.1	5.9	39.2	20.6
4515.698.....	0.600	0.627	0.329	-52.8	-65.0	-26.5	-56.7
4516.680.....	0.600	0.802	0.332	-92.7	-89.6	-82.7	-91.4
4854.722.....	0.600	0.169	0.482	128.1	122.1	137.9	133.0
4855.822.....	0.600	0.366	0.486	42.7	47.4	55.1	65.3
4856.838.....	0.600	0.547	0.489	-17.9	-22.5	-28.6	-9.0
4857.818.....	0.600	0.722	0.493	-98.3	-96.1	-71.9	-94.8
4858.810.....	0.600	0.899	0.496	-93.4	-60.9	-69.2	-67.6
4860.853.....	0.600	0.264	0.503	53.8	67.5	93.9	71.9
5098.705.....	0.600	0.740	0.312	-81.4	-77.3	-50.3	-70.7
5099.716.....	0.600	0.921	0.315	-43.1	-30.1	-26.6	-28.9
5142.843.....	0.600	0.622	0.462	-47.5	-39.1	-47.3	-41.8
5143.852.....	0.600	0.802	0.465	-85.8	-72.2	-70.1	-70.5
5144.839.....	0.600	0.978	0.469	-29.3	-26.1	-13.3	-22.7
5145.855.....	0.600	0.160	0.472	55.1	54.5	74.3	70.5
5186.793.....	0.600	0.470	0.612	7.7	13.0	11.4	21.9
5187.828.....	0.600	0.655	0.615	-70.6	-60.0	-66.7	-61.9
5188.767.....	0.600	0.823	0.618	-66.8	-74.3	-55.9	-61.0
5188.869.....	0.600	0.841	0.619	-64.8	-70.5	-55.1	-61.1
5188.953.....	0.600	0.856	0.619	-63.1	-65.3	-55.3	-54.2
5189.793.....	0.600	0.006	0.622	-7.3	-10.1	11.2	4.0
5190.762.....	0.600	0.179	0.625	52.9	56.5	52.9	47.9
5190.901.....	0.600	0.204	0.626	69.7	66.0	75.2	67.9
5241.707.....	0.600	0.277	0.798	70.3	74.8	83.7	62.9
5242.669.....	0.600	0.449	0.802	14.3	10.5	26.7	11.4
5242.767.....	0.600	0.466	0.802	-20.9	-2.9	18.8	-1.8
5243.697.....	0.600	0.632	0.805	-80.5	-78.7	-94.0	-73.9
5262.657.....	0.600	0.019	0.870	0.3	-3.0	7.6	2.0
5512.799.....	0.600	0.689	0.720	-79.2	-78.0	-61.8	-62.9
5512.941.....	0.600	0.714	0.721	-77.5	-86.1	-53.5	-61.5
5513.822.....	0.600	0.871	0.724	-66.4	-66.0	-46.6	-57.0
5515.875.....	0.600	0.238	0.731	76.3	70.9	79.0	80.5
5544.773.....	0.600	0.398	0.829	28.2	37.2	50.1	45.3
5544.907.....	0.600	0.422	0.830	26.4	31.5	47.4	40.2
5545.724.....	0.600	0.568	0.832	-41.6	-30.9	-31.7	-24.7
5545.886.....	0.600	0.597	0.833	-46.0	-36.5	-35.2	-37.2
5546.774.....	0.600	0.756	0.836	-90.5	-75.9	-76.1	-68.6
5546.914.....	0.600	0.781	0.836	-92.1	-82.4	-80.4	-75.7
5547.856.....	0.600	0.949	0.840	-37.8	-42.8	-42.8	-35.7
DAO 1.83 m:							
5667.635.....	0.465	0.340	0.247	49.7	70.6	108.2	77.0
5668.624.....	0.465	0.516	0.250	-27.6	-9.3	12.8	6.5
5669.635.....	0.465	0.697	0.254	-99.6	-80.2	-55.6	-73.4
5670.615.....	0.465	0.872	0.257	-60.6	-53.3	-31.1	-62.0
5687.627.....	0.465	0.910	0.315	-60.8	-55.7	-48.2	-49.2
DAO 1.22 m:							
5888.782.....	0.600	0.831	0.999	-84.5	-74.6	-72.6	-71.5
5888.891.....	0.600	0.851	0.000	-64.9	-65.9	-67.6	-61.7
5889.807.....	0.600	0.014	0.003	-11.6	-5.7	7.1	-2.8
5889.904.....	0.600	0.032	0.003	-1.1	5.7	14.2	6.4
5890.794.....	0.600	0.191	0.006	71.5	68.7	76.9	64.7
5890.895.....	0.600	0.209	0.006	73.5	68.6	69.1	76.3
5891.799.....	0.600	0.370	0.010	47.5	55.3	67.1	61.6
5891.897.....	0.600	0.388	0.010	59.2	50.6	66.5	56.0
5892.800.....	0.600	0.549	0.013	-24.6	-23.7	-14.7	-8.5
5892.897.....	0.600	0.566	0.013	-26.6	-31.6	-20.3	-19.8
5893.878.....	0.600	0.741	0.017	-86.9	-85.1	-67.8	-74.1
5894.795.....	0.600	0.905	0.020	-61.7	-52.4	-48.2	-47.3

TABLE 1—Continued

BJD 2,440,000+	Dispersion (Å per diode)	5.6 Day Binary Phase	294 Day X-Ray Phase	H (km s <sup>-1</sup> )	He I (km s <sup>-1</sup> )	He II (km s <sup>-1</sup> )	Metal (km s <sup>-1</sup> )
CFHT 3.6 m:							
5889.854.....	0.036	0.023	0.003	...	2.4	...	...
5889.983.....	0.036	0.046	0.003	...	16.3	...	...
5890.072.....	0.036	0.062	0.004	...	24.2	...	...
5890.857.....	0.036	0.202	0.006	...	61.2	...	...
5890.959.....	0.036	0.220	0.007	...	71.6	...	...
5891.051.....	0.036	0.237	0.007	...	71.8	...	...
5891.938.....	0.036	0.395	0.010	...	49.6	...	...
5892.023.....	0.036	0.410	0.010	...	49.9	...	...
5892.105.....	0.036	0.425	0.011	...	38.7	...	...
5892.854.....	0.036	0.558	0.013	...	-24.1	...	...
5892.940.....	0.036	0.574	0.013	...	-29.6	...	...
5893.078.....	0.036	0.599	0.014	...	-41.5	...	...
5893.824.....	0.036	0.732	0.016	...	-73.7	...	...
5893.947.....	0.036	0.754	0.017	...	-75.4	...	...
5894.059.....	0.036	0.774	0.017	...	-73.4	...	...
Centered at H $\alpha$							
DAO 1.83 m:							
5887.807.....	0.231	0.663	0.996	...	-61.6	...	...
5888.800.....	0.231	0.834	0.999	...	-66.8	...	...
5888.893.....	0.231	0.851	0.000	...	-60.2	...	...
5889.894.....	0.231	0.031	0.003	...	-6.4	...	...
5890.805.....	0.231	0.193	0.006	...	63.9	...	...
5890.895.....	0.231	0.209	0.006	...	64.9	...	...
5891.797.....	0.231	0.370	0.010	...	56.8	...	...
5891.891.....	0.231	0.386	0.010	...	47.8	...	...
5892.789.....	0.231	0.547	0.013	...	-33.4	...	...
5892.895.....	0.231	0.565	0.013	...	-34.2	...	...
5893.810.....	0.231	0.729	0.016	...	-78.4	...	...
5894.802.....	0.231	0.906	0.020	...	52.0	...	...
5895.791.....	0.231	0.083	0.023	...	19.2	...	...
5895.895.....	0.231	0.102	0.023	...	28.2	...	...

NOTE.—Errors in the DAO 1.22 m velocities are  $\pm 2$  km s<sup>-1</sup> for the He II and H lines and  $\pm 1$  km s<sup>-1</sup> for the He I and metal lines. Errors in the CFHT 3.6 m and DAO 1.83 m velocities are  $\pm 1$  km s<sup>-1</sup> and  $\pm 2$  km s<sup>-1</sup>, respectively.

are identified in Table 2. The identifications are based on the wavelengths for stellar lines given by Moore (1959), the night-sky lines are taken from Meinel, Aveni, and Stockton (1975), and the interstellar lines from Herbig (1975) and Scholz (1972). The plethora of lines shortward of H $\alpha$  in the third box of Figure 1 is from telluric water vapor.

Apart from the peculiar emission of He II at  $\lambda 4686$ , the spectrum of HDE 226868 is typical for a star with a spectral type of O9.7 Iab (Walborn 1973). We found no significant difference in the strength of the metal lines compared to single stars of the same spectral type, as would be the case if significant mass loss from the primary had affected relative abundances (Dearborn and Eggleton 1977).

A number of lines do not appear to have been noticed in the literature previously. The weak interstellar feature seen at  $\lambda 4963$  in Figure 1 stands out in the spectrum of HDE 226868 as it does not share in the large velocity variations associated with the binary motion. This line was also seen in high signal-to-noise ratio Reticon spectra of two other strongly reddened early-type stars, HD 206267 and HD 207198. The unidentified emission lines at  $\lambda 6667$  and  $\lambda 6700$  in the spectrum of 19 Cephei in Figure 1 are discussed in another paper (Ninkov *et al.* 1987).

### III. THE ORBIT

Using the iron-argon hollow-cathode lamp for wavelength calibration, velocities were measured for all of the lines listed in

Table 3. The position of each line was estimated using a center-of-weight criterion, with the estimated line position given by  $\sum I_j p_j / \sum I_j$ , where  $p_j$  is the position of the pixel in the line profile and  $I_j$  is the associated intensity relative to the continuum at that pixel. The summation was performed over a consistent estimate of the line limits which, in our case, were chosen as the half-intensity points.

In Table 1, mean weighted radial velocities of lines in the H, He I, He II, and metal (Si, C, N, and O) groups (listed in Table 3), are listed for each spectrum, together with the corresponding epoch of observation. All the lines in each of the four groups were assigned a weight which depended on the strength of the line and its position in the spectrum. When calculating mean group velocities, the weights allow for the effect of line blending and the lower signal to noise towards the edge of the Reticon spectra. The weights are listed in Table 3 together with the excitation potential (=ionization potential of the lower ionization level + excitation potential of the lower line level) of the ion responsible for the line (Hutchings 1976).

Based on multiple spectra of brighter stars, the  $\sigma$  errors in the radial velocities for the DAO and CFHT observations are 4 km s<sup>-1</sup> and 1 km s<sup>-1</sup> per line, respectively. The velocities listed in Table 1 have been corrected to the solar system barycenter using algorithms from Stumpff (1979). For the 1984 DAO 1.83 m red data, only the He I  $\lambda 6678$  line could be measured.

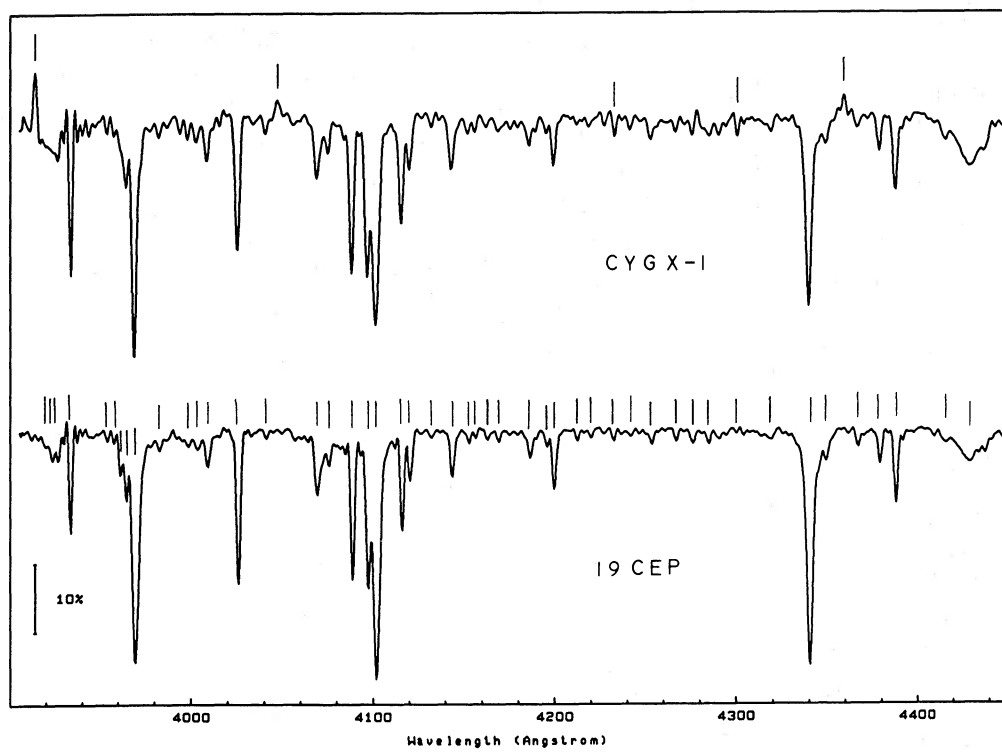


FIG. 1a

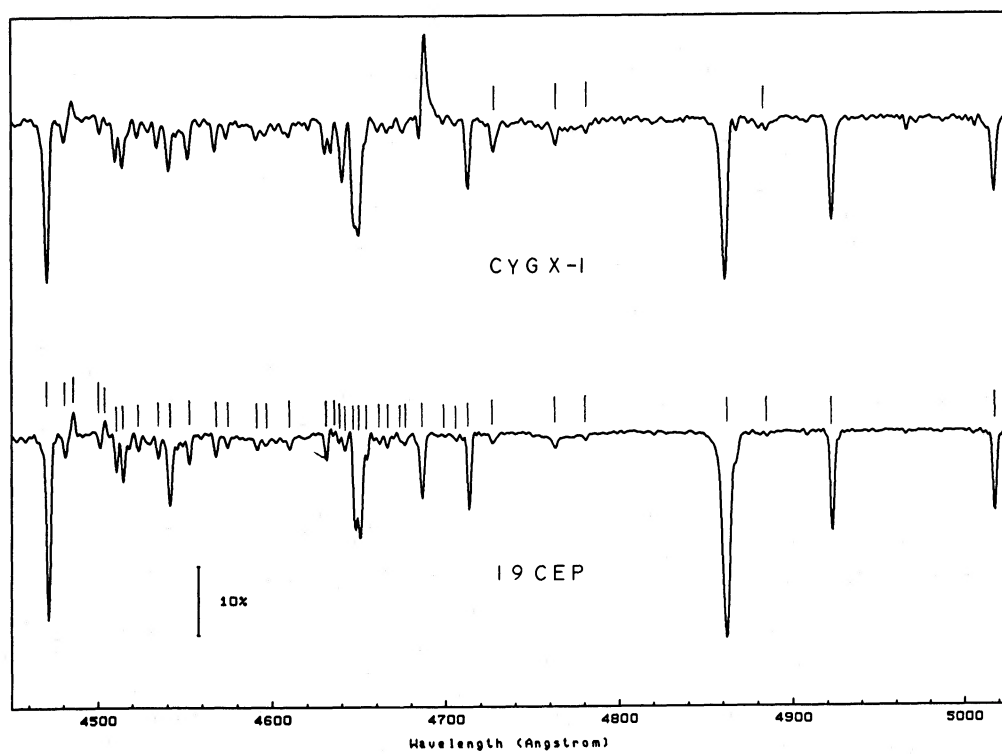


FIG. 1b

FIG. 1.—The spectrum of Cyg X-1 (*upper*) and 19 Cep (*lower*) taken at  $40 \text{ \AA mm}^{-1}$ . Tick marks on lower plot indicate identified (Table 2) stellar lines and those on upper plot indicate interstellar and night-sky lines. Resolution is  $\sim 1.2 \text{ \AA}$  in blue spectra and  $\sim 0.5 \text{ \AA}$  for the red spectra.

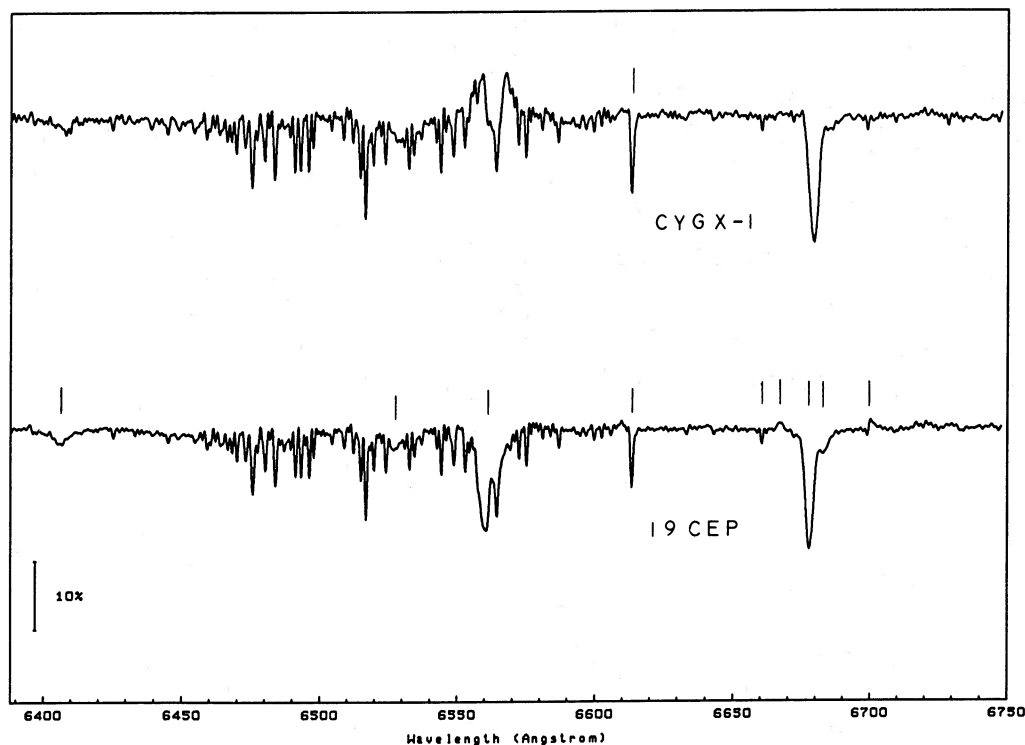


FIG. 1c

The orbital period was determined from the observations in Table 1 to be  $5.60172 \pm 0.00003$  days using the period-folding technique of Morbey (1978). The accuracy of this period is limited by phase errors in the timing of the center point of individual observations which were typically 3 hr exposures. No significant period was found when the data was folded on periods near the 294 day X-ray period of Priedhorsky, Terrell, and Holt (1983). In order to improve the search for any long-period variations, all historic velocity measures (Seyfert and Popper 1941; Webster and Murdin 1972; Brucato and Kristian 1973; Smith, Margon, and Conti 1973; Brucato and Zappala 1974; Mason *et al.* 1974; Abt, Hintzen, and Levy 1977; Gies and Bolton 1982) were combined and an orbital period of  $5.59964 \pm 0.00001$  days was found using period folding. No periodicities were found corresponding to the 294 day X-ray period (Priedhorsky, Terrell, and Holt 1983) or the 39/78 day polarization period (Kemp, Herman, and Barbour 1978) or to the 91 day photometric period (Walker and Quintanilla 1978).

Our velocities were used for a single-line binary solution following the procedure of Herbison-Evans and Lomb (1971). The solutions to the mean H, He I, He II, and metal-line velocities are given in Table 4 along with the standard deviation ( $\sigma$ ) of the solution to the data points. An example of the fit is illustrated for the He I data in Figure 2. The best solution for each of the lines was found with the eccentricity close to zero. These small nonzero eccentricities had a significance  $< 5\%$  according to the Lucy and Sweeney (1971) criterion. Thus for the orbital solutions presented in Table 4, the  $K$  and  $V_0$  were determined with the eccentricity set to zero, and the period and  $T_0$  were held constant (indicated by square brackets) at the values found from our period folding analysis. The latter ephemeris was used to calculate the binary phases given in the fluid column of Table 1. The fourth column of Table 1 contains

phases determined from the ephemeris for the 294 day X-ray modulation given by Priedhorsky, Terrell, and Holt (1983). The zero of the 294 day X-ray phase corresponds to a minimum in the X-ray flux.

Our orbital solutions in Table 4 are very similar to those of Gies and Bolton (1982) and, for comparison, their solution for He I is given in the final column of Table 4. Our  $K$  values for different ions agree to within the error bars with Gies and Bolton (1982) and we (both) find essentially zero eccentricity. The  $V_0$  values presumably differ between species because they are formed in different parts of the expanding stellar wind. This causes a systematic decrease in  $V_0$  in the sequence of solutions from He II (high-excitation energy), metal lines, He I to H I (low-excitation energy). Our values of  $V_0$  are similar to those found by Gies and Bolton (1982) for the He I lines but differ for the H I Balmer lines.

The periods determined for the system based on our data alone and together with the literature data differ by 0.00206 days (5.60172 vs. 5.59964 days) which is 20 times the standard deviation in the period found for the former. To investigate this discrepancy a least-squares fit of the orbital solution was made to the observed velocities at each epoch. The orbital solution used was

$$V_i = K \sin [2\pi(T_i - T_0 + \delta T_0)/\text{period}] ; \quad (1)$$

the constants were taken from our He I velocity observations, i.e.,  $K = 75 \text{ km s}^{-1}$ ,  $T_0 = 2441869.17$ , period = 5.59964 days, and  $\delta T_0$  is the free parameter. Some of the literature velocity values were from lines other than He I. In such cases, these velocities were offset by an amount equal to the difference in  $V_0$  found for that ion compared to He I in Table 4. The free parameter is  $\delta T_0$ , and we look for systematic variations in  $\delta T_0$  which might have been introduced by assuming a constant period. Table 5 lists the values of  $\delta T_0$  found from a best-fit of

TABLE 2  
LINES IDENTIFIED IN THE SPECTRA OF HDE 226868 AND 19 CEPHEI

Line	Wavelength (Å)	Line	Wavelength (Å)
N <sub>2</sub> (Aurora) .....	3914.4	He I .....	4387.928
O II .....	3919.29	O II .....	4414.909
He II .....	3923.48	? (IS) .....	4428.0
He I .....	3926.530	He I .....	4471.477
Ca II (IS) .....	3933.64	Mg II .....	4481.228
O II .....	3954.370	? .....	4485.7
O II .....	3961.59	? (IS) .....	4501.8
He I .....	3964.727	? .....	4503.7
Ca II (IS) .....	3968.470	N III .....	4510.92
He .....	3970.074	N III .....	4514.89
O II .....	3982.72	He II .....	4541.59
N III .....	3998.69	Si III .....	4522.654
N III .....	4003.64	Si III .....	4567.872
He I .....	4009.270	Si III .....	4574.777
He I .....	4026.189	O II .....	4590.971
N II .....	4035.087	O II .....	4596.17
Hg I (NS) .....	4047.0	N II .....	4613.87
O II .....	4069.897	N II .....	4630.537
O II .....	4075.86	N II .....	4634.16
Si IV .....	4088.863	O II .....	4638.85
N III .....	4097.31	N III .....	4640.64
Hδ .....	4101.737	C III .....	4647.40
Si IV .....	4116.104	O II .....	4650.84
He I .....	4120.812	Si IV .....	4654.32
O II .....	4132.81	O II .....	4661.635
He I .....	4143.759	O II .....	4673.75
O II .....	4153.30	O II .....	4676.234
Blend .....	4156.7	He II .....	4685.682
C III .....	4162.86	O II .....	4699.21
He I .....	4168.97	O II .....	4705.355
O II .....	4185.456	He I .....	4713.143
N III .....	4195.70	? (IS) .....	4726
He II .....	4199.83	? (IS) .....	4763.0
S III .....	4211.68	? (IS) .....	4779.7
Ne II .....	4219.76	Hβ .....	4861.332
CH <sup>+</sup> (IS) .....	4232.6	? (IS) .....	4882.0
N II .....	4241.787	He I .....	4921.929
O II .....	4253.74	? (IS) .....	4963.0
C II .....	4267.02	He I .....	5015.675
C II .....	4267.27	He I .....	5047.736
O II .....	4276.21	He II .....	6406.3
Si III .....	4284.99	He II .....	6527.3
CH (IS) .....	4300.6	Hα .....	6562.817
O II .....	4319.93	? (IS) .....	6613.63
Hγ .....	4340.468	? (IS) .....	6660.71
O II .....	4349.426	? .....	6667.0
Hg I (NS) .....	4358.3	He I .....	6678.149
O II .....	4366.896	? .....	6700.0
N III .....	4379.09	He II .....	6683.2

TABLE 3  
LINE WEIGHTS FOR THE LEAST-SQUARES FITTING OF THE RADIAL  
VELOCITY CURVE IN EACH LINE GROUP

Line	Wavelength	Excitation Potential in eV (weighted means in parentheses)	Weight
Hydrogen:			
Hδ .....	4101.737	10	0.5
Hγ .....	4340.468	10	1.0
Hβ .....	4861.332	10	0.8
Weighted mean .....		(10)	
He I .....			
He I .....	4009.270	21	0.1
He I .....	4026.189	21	0.8
He I .....	4120.812	21	0.4
He I .....	4143.759	21	0.8
He I .....	4387.928	21	0.8
He I .....	4471.477	21	1.0
He I .....	4713.143	21	1.0
He I .....	4921.929	21	0.8
He I .....	5015.675	21	0.8
He I .....	5047.736	21	0.5
Weighted mean .....		(21)	
He II .....			
He II .....	4199.83	75	0.4
He II .....	4541.598	75	0.4
He II .....	4685.685	75	1.0
Weighted mean .....		(75)	
Metal:			
O II .....	4069.897	36	0.2
O II .....	4075.86	36	0.1
Si IV .....	4088.863	57	1.0
N III .....	4097.31	57	0.4
Si IV .....	4116.104	57	0.8
O II .....	4349.426	36	0.1
O II .....	4366.896	36	0.1
N III .....	4379.09	57	0.8
Mg II .....	4481.228	8.5	0.6
N III .....	4510.92	57	0.5
N III .....	4514.89	57	0.5
Si III .....	4552.654	57	0.5
Si III .....	4567.872	57	0.5
Si III .....	4574.777	57	0.1
N II .....	4630.537	35	0.1
N III .....	4634.16	57	0.2
N III .....	4640.64	57	0.5
C III .....	4647.40	54	0.2
O III .....	4650.74	36	0.2
Weighted mean .....		(50)	

TABLE 4

HDE 226868 ORBIT SOLUTIONS FOR GROUPS OF LINES WITH DIFFERENT EXCITATION ENERGIES (LISTED IN TABLE 2)

Element	H	He I	He II	Metal	He I (Gies and Bolton)
Period (d) .....	[5.6017]	5.6017(1)	[5.6017]	[5.6017]	5.59974
T <sub>0</sub> (2,440,000+) .....	[1869.17]	1869.17(1)	[1869.17]	[1869.17]	1869.110
V <sub>0</sub> (km s <sup>-1</sup> ) .....	-9.15(70)	-4.44(50)	6.27(70)	0.10(70)	-3.7
K (km s <sup>-1</sup> ) .....	78.1(16)	75.0(10)	75.4(20)	75.9(15)	73.3
e .....	0.0	0.0	0.0	0.0	0.0
σ fit (km s <sup>-1</sup> ) .....	6.5	6.2	9.5	5.6	7.7

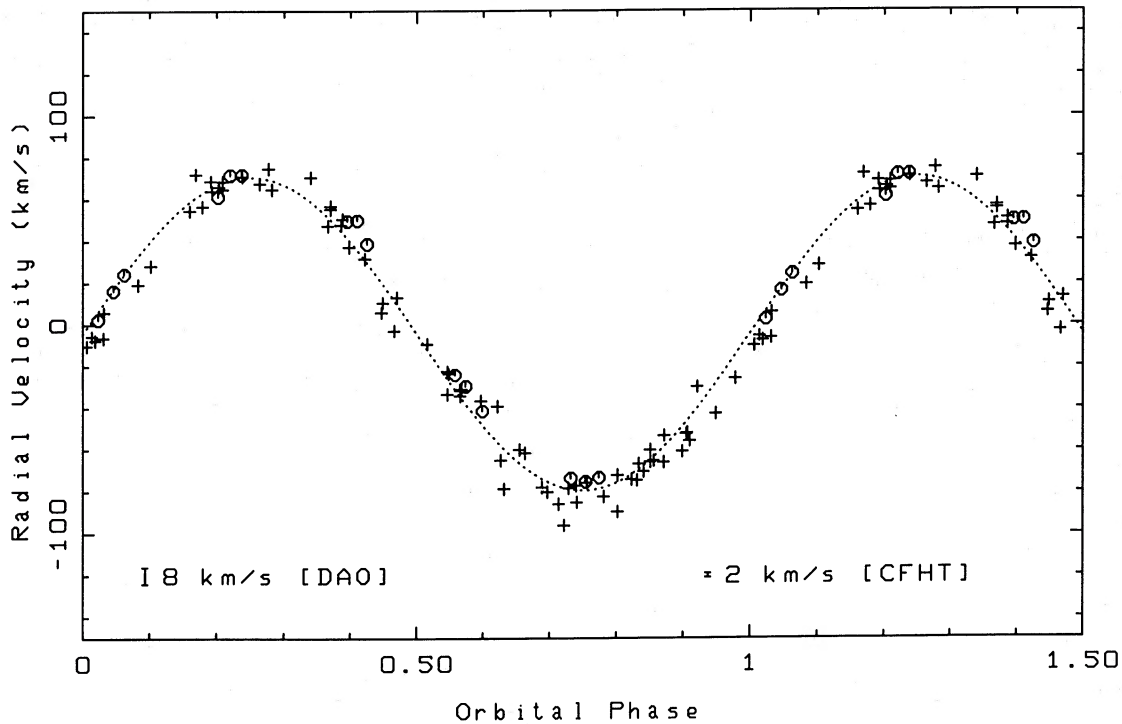


FIG. 2.—Mean He I line radial velocity curve for HDE 226868. Crosses denote data from DAO, circles indicate CFHT data, dotted curve is best orbital solution to the data as given in Table 3. The  $2\sigma$  error bars are indicated.

solution (1) to the data at the epochs indicated, along with the number of velocity data points available for the fit at each epoch. Figure 3 shows  $\delta T_0$  as a function of epoch, along with a weighted (by the number of velocity measurements at each epoch) linear fit to the data. According to Batten (1973) for real period changes, the plots should show a curved line, while a positive, straight line indicates an assumed period which is too short.

Figure 3 does not give a clear answer to the question of period change. At face value, the linear fit indicates that the period is too short. However, the data points, by eye, seem to be constant at epochs before 2,444,513.70 and positive after this epoch. Additional observations in  $\sim 5$ – $10$  yr time should clearly answer whether the period is changing or not.

#### IV. $v \sin i$

Following the technique of Ebbets (1979) and Gray (1976)  $v \sin i$  was determined from the first zero in the Fourier transform of the line profile using the high-resolution ( $0.036 \text{ \AA}$  per diode) CFHT data of the He I  $\lambda 4713$  line. As a test we found the technique gave accurate values of  $v \sin i$  for theoretically broadened profiles (of known  $v \sin i$ ) from Stoeckley and Mihalas (1973) and gave  $v \sin i = 75.1 \text{ km s}^{-1}$  for 19 Cep, which is close to the  $72 \text{ km s}^{-1}$  determined by Ebbets (1979). The  $v \sin i$  estimated for HDE 226868 by this technique is  $94.3 \pm 5 \text{ km s}^{-1}$  which differs significantly from the value of  $140 \text{ km s}^{-1}$  determined by Bolton (1975) but agrees with the more recent value of  $96 \text{ km s}^{-1}$  measured by Gies and Bolton (1986).

Figure 4 shows the HDE 226868 He I  $\lambda 4713$  profile (dashed) along with a series of theoretical profiles for a star of  $\log g = 3.0$ ,  $T = 27,500 \text{ K}$  from Stoeckley and Mihalas (1973) for different values of  $v \sin i$ . The observed profile agrees well with a theoretical one having  $v \sin i$  of  $100 \text{ km s}^{-1}$  of 100

$\text{km s}^{-1}$ . Small errors ( $< 5\%$ ) in the assumed position of the continuum of HDE 226868 do not seriously change the estimated value of  $v \sin i$ .

#### V. ABSOLUTE MAGNITUDE AND DISTANCE

Walker and Millward (1985) calibrated the variations of equivalent width of  $H\gamma$  with absolute magnitude for early-type supergiants in  $h$  and  $\chi$  Per. The calibration has been confirmed and extended to the O supergiants by Hill, Walker, and Yang (1986). Using the criteria of Walker and Millward (1985) for avoiding the effect of line blends in  $H\gamma$ , we measured an equivalent width for  $H\gamma$  of  $1.5 \pm 0.1 \text{ \AA}$  from spectra of HDE 226868 taken in 1982 August. Their calibration leads to an absolute magnitude of  $-6.5 \pm 0.2$  which is close to the canonical value of  $-6.4$  for spectral class O9.7 Iab (Schmidt-Kaler 1982).

Adopting a value for  $E(B-V)$  ranging from 1.12 (Bregman *et al.* 1973) to 0.95 (Wu *et al.* 1982), for  $R = 3.2$  (Seaton 1979), and a  $V$  apparent magnitude of  $8.89 \pm 0.02$  (Beall *et al.* 1984) and using  $M_v = -6.5 \pm 0.2$  leads to a distance for HDE 226868 of  $2.5 \pm 0.3 \text{ kpc}$ . Margon, Bowyer, and Stone (1973) and Bregman *et al.* (1973) determined the reddening as a function of distance in the direction of Cyg X-1 using nearby field stars. From the known reddening to Cyg X-1, they inferred a distance of  $> 2 \text{ kpc}$ , which is compatible with our value. Cyg X-1 lies only  $1^\circ$  from the center of NGC 6871, the core of the Cyg OB3 association, which has a photometric distance of  $1.8 \pm 0.5 \text{ kpc}$  (Janes and Adler 1982). The association of Cygnus X-1 with NGC 6871 remains tenuous, however, because of the disparity in the distances ( $2.5 \pm 0.3 \text{ kpc}$  vs.  $1.8 \pm 0.3 \text{ kpc}$ ). Taking the lower limit to the distance to Cygnus X-1 of  $d = 2.2 \text{ kpc}$ , estimated above from  $H\gamma$ , gives a minimum secondary mass of  $4 M_\odot$  according to Paczyński (1974).

TABLE 5  
 FITTED  $\delta T_0$  VALUES FOR ALL VELOCITY DATA ON CYGNUS X-1

Mean epoch of observation (JD)	Number of observations	$\delta T_0$ (days)	Source of Data
2429664.2200	2	-0.968	Seyfert and Popper (1941)
2441207.4305	4	-0.235	Webster and Murdin (1972)
2441233.6543	7	-0.137	Webster and Murdin (1972)
2441215.0783	3	-0.127	Brucato and Kristian (1973)
2441476.8595	4	-0.003	Brucato and Kristian (1973)
2441495.8498	5	-0.023	Smith <i>et al.</i> (1973)
2441587.7885	2	+0.067	Smith <i>et al.</i> (1973)
2441859.7022	13	+0.007	Brucato and Zappala (1974)
2441919.7360	3	+0.002	Brucato and Zappala (1974)
2441269.7975	2	-0.079	Mason <i>et al.</i> (1974)
2441400.3493	3	-0.037	Mason <i>et al.</i> (1974)
2441424.1528	4	+0.061	Mason <i>et al.</i> (1974)
2441453.5910	2	-0.343	Mason <i>et al.</i> (1974)
2441525.4365	2	-0.698	Mason <i>et al.</i> (1974)
2441935.0195	2	+0.092	Mason <i>et al.</i> (1974)
2442205.854	5	+0.038	Abt <i>et al.</i> (1977)
2442229.4679	18	+0.086	Abt <i>et al.</i> (1977)
2442257.7712	4	-0.006	Abt <i>et al.</i> (1977)
2442266.3144	7	-0.052	Abt <i>et al.</i> (1977)
2442286.8819	35	+0.033	Abt <i>et al.</i> (1977)
2442680.3177	6	+0.087	Abt <i>et al.</i> (1977)
2442909.6020	6	+0.053	Abt <i>et al.</i> (1977)
2441225.1380	2	-0.216	Gies and Bolton (1982)
2441257.8820	3	-0.161	Gies and Bolton (1982)
2441464.7885	4	-0.010	Gies and Bolton (1982)
2441535.1965	2	-0.071	Gies and Bolton (1982)
2441893.1980	6	-0.065	Gies and Bolton (1982)
2441929.9543	3	-0.032	Gies and Bolton (1982)
2442306.1300	2	-0.129	Gies and Bolton (1982)
2442542.7823	3	-0.045	Gies and Bolton (1982)
2443342.7575	2	+0.029	Gies and Bolton (1982)
2443373.6688	4	+0.111	Gies and Bolton (1982)
2444058.3552	13	+0.088	Gies and Bolton (1982)
2444795.0557	3	+0.131	Gies and Bolton (1982)
2444514.7178	3	-0.057	this work
2444858.0783	4	+0.120	this work
2445099.2101	2	-0.007	this work
2445144.3448	4	+0.103	this work
2445189.0799	8	+0.224	this work
2445243.0424	3	-0.125	this work
2445513.3080	2	+0.145	this work
2445545.9832	6	+0.183	this work
2445669.6208	2	+0.145	this work
2445891.2030	11	+0.231	this work
2445891.9116	15	+0.230	this work
2445892.1149	13	+0.188	this work

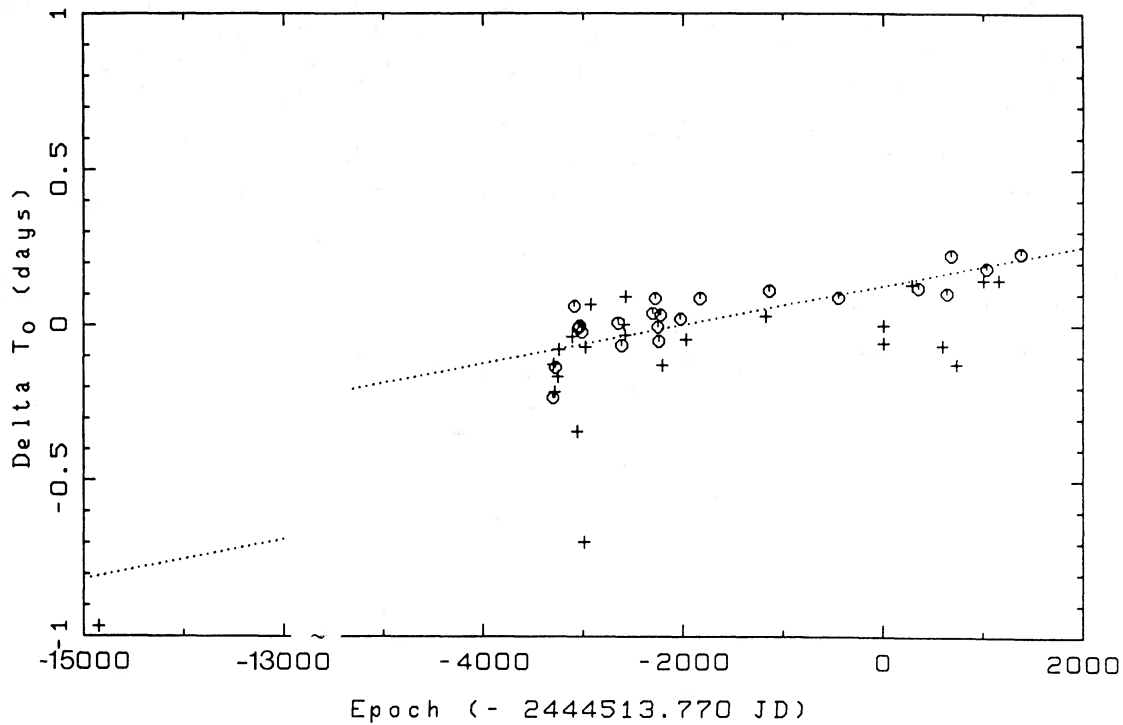


FIG. 3.—Fitted values of  $\delta T_0$  vs. epoch of observation for all velocity measures of Cyg X-1 (1939–1984). Crosses and circles indicate two and more than two observations, respectively, used to find  $\delta T_0$  at a particular epoch. The weighted least-squares fit to the data, not using the 1939/1940 historical data point is  $\delta T_0 = 0.12(08) + 5.7(3.7) \times 10^{-5}T$ , where  $T$  is the epoch of observation and the numbers in brackets reflect the uncertainties in the fit.

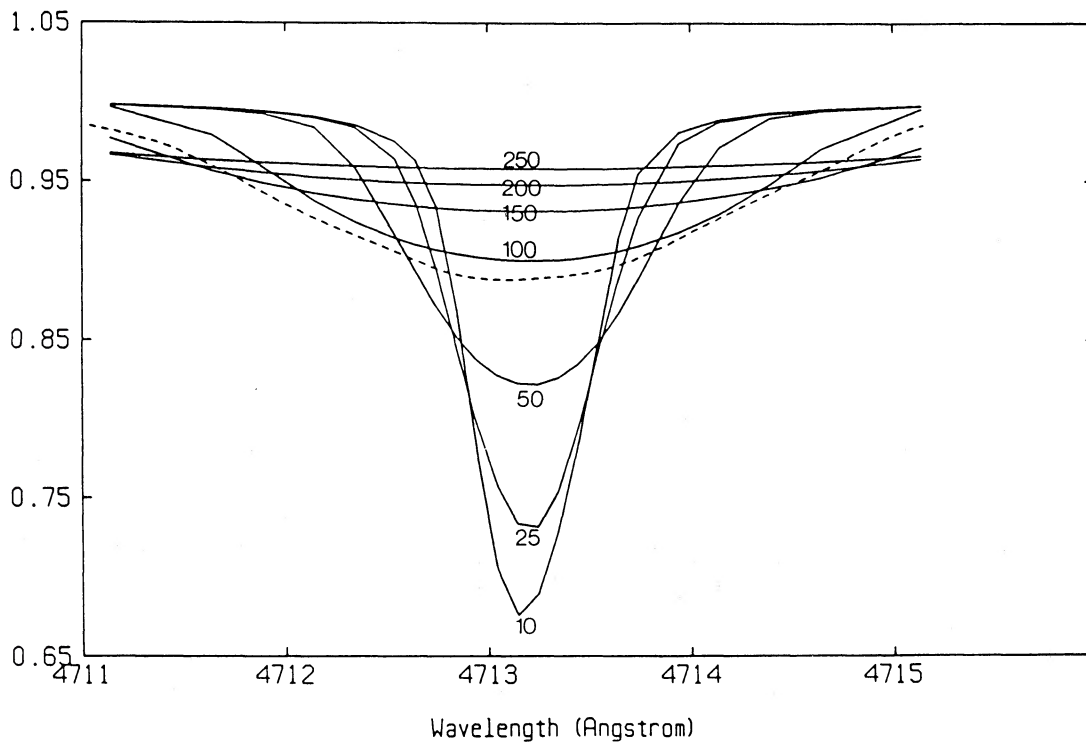


FIG. 4.—He I  $\lambda 4713$  profile at CFHT (*dashed*) together with profiles from Stoeckley and Mihalas (1973) (*solid*) for the range of  $v \sin i$  labeled (in  $\text{km s}^{-1}$ ). Continuum = 1.0.

## VI. EQUIVALENT WIDTHS

Equivalent widths were measured for most lines listed in Table 2. These values, normalized with respect to the mean value of each line, were binned in 0.1 phase bins (the third through twelfth columns) and are listed in Table 6. No systematic variation was found corresponding to the 5.6 day orbital period.

In order to search for variations in  $v \sin i$  the half-widths of

the He I  $\lambda 4471$  and  $\lambda 4713$  were measured for both HDE 226868 and 19 Cep on each night they were both observed. The ratio of the half-widths (HDE 226868/19 Cep) was used to eliminate potential instrumental variations, since the 19 Cep profile is not expected to vary intrinsically. The ratios have an average uncertainty of  $\pm 3\%$  and are listed in Table 7 in bins of 0.1 orbital phase. No variation was found. Sokolov and Tsymbal (1984) and Kopylov and Sokolov (1984)

TABLE 6  
HDE 226868 EQUIVALENT WIDTH VARIATIONS WITH ORBITAL PHASE NORMALIZED WITH RESPECT TO MEAN

Line $\text{\AA}$	Mean EW (m $\text{\AA}$ )	Orbital Phase Bins									
		0.0- 0.1	0.1- 0.2	0.2- 0.3	0.3- 0.4	0.4 0.5	0.5- 0.6	0.6- 0.7	0.7- 0.8	0.8- 0.9	0.9- 1.0
<u>Hydrogen</u>											
4340.468	1745	1.14	1.05	0.97	1.09	0.93	0.92	0.91	1.01	1.02	1.00
4861.332	1232	1.01	0.98	1.02	1.03	0.95	0.96	0.93	1.03	1.02	0.98
<u>He I</u>											
4026.189	547	1.06	1.00	1.00	0.96	0.99	1.04	0.97	1.04	0.99	0.98
4120.812	233	1.02	1.11	0.91	0.92	0.97	1.03	0.98	1.11	0.97	1.00
4143.759	237	1.03	1.04	0.96	0.94	1.01	1.02	1.02	1.02	0.93	1.04
4387.928	318	1.09	0.96	0.97	1.02	1.02	0.99	0.96	1.04	1.01	0.95
4471.477	645	1.03	0.98	0.96	0.99	1.00	1.01	0.99	1.03	1.01	1.01
4713.143	273	1.07	0.98	0.96	1.00	1.01	1.01	0.99	1.03	0.98	0.98
4921.929	406	1.05	0.99	0.98	0.93	1.07	0.96	0.96	1.07	0.98	0.99
5015.675	292	1.06	0.98	1.03	0.98	1.04	0.97	0.96	1.05	0.94	0.99
<u>He II</u>											
4199.83	194	1.03	1.07	0.99	0.94	1.00	0.97	1.07	0.98	1.05	1.02
4541.598	191	0.95	1.03	0.93	1.05	1.07	1.01	0.93	1.09	0.96	0.99
<u>Metal</u>											
4069.897	243	1.05	1.01	0.88	1.05	1.05	0.89	0.98	1.08	0.99	1.03
4075.86	164	0.97	1.10	1.01	0.89	0.96	1.02	1.03	0.97	0.92	1.10
4088.863	599	0.99	0.96	1.01	1.01	0.99	1.02	0.97	1.07	1.03	0.96
4097.31	629	1.03	1.00	1.00	0.94	1.00	0.97	0.98	1.09	1.00	1.00
4116.104	434	1.05	1.02	0.90	0.94	0.98	1.04	0.98	1.12	0.98	1.01
4379.09	149	1.10	1.09	0.90	1.10	1.05	0.96	0.88	1.01	0.97	0.96
4481.228	91	0.96	1.00	0.91	1.00	1.01	1.10	1.04	0.98	0.98	1.02
4510.92	142	0.94	0.93	0.91	1.07	0.96	1.01	1.06	1.05	1.05	1.03
4514.89	176	0.96	0.89	0.88	1.05	1.02	1.04	0.98	1.11	1.03	1.04
4552.654	164	1.06	0.98	0.98	0.98	0.99	0.96	1.00	1.09	0.90	1.06
4630.537	130	1.02	1.01	0.99	0.96	0.99	1.00	0.99	1.10	1.05	1.01
4634.16	132	0.98	1.09	1.02	0.94	1.00	0.93	0.90	1.05	1.14	0.95
4640.64	238	1.09	1.00	0.96	0.99	0.96	0.98	1.00	1.07	1.05	1.07
4647.40	418	1.08	0.97	0.95	1.00	1.00	0.97	0.95	1.00	1.04	1.04
4650.74	447	1.04	1.06	1.00	0.94	1.03	0.96	0.99	0.98	1.01	0.98
<u>IS</u>											
3933.64	572	1.04	1.02	0.93	0.98	0.98	1.02	0.98	0.95	1.09	1.03
4726.0	133	1.06	0.99	0.99	1.00	0.97	1.02	1.03	0.99	0.98	1.00
4763.0	106	0.96	0.99	1.01	0.96	1.01	0.96	1.08	0.99	1.05	1.00

TABLE 7  
RATIO OF He I HALF-WIDTHS IN HDE 226868 TO  
19 CEPHEI AS A FUNCTION OF THE 5.6 DAY  
ORBITAL PHASE

Phase Bin	He I $\lambda 4713$ (Cyg X-1/19 Cep)	He I $\lambda 4471$ (Cyg X-1/19 Cep)
0.0-0.1.....	1.13	1.15
0.1-0.2.....	1.13	1.16
0.2-0.3.....	1.10	1.11
0.3-0.4.....	1.12	1.12
0.4-0.5.....	1.14	1.09
0.5-0.6.....	1.15	1.13
0.6-0.7.....	1.12	1.10
0.7-0.8.....	1.17	1.16
0.8-0.9.....	1.16	1.15
0.9-1.0.....	1.12	1.15

NOTE.—Error in the ratio for any bin  $\approx \pm 0.03$ .

find from long-term  $U$ ,  $B$ ,  $V$  variability and differences in  $v \sin i$  measures that the inclination of HDE 226868 varies with an amplitude of  $16^\circ$  (they assumed an inclination of  $30^\circ$ ) over a period of 39 days. Such a change in the inclination would imply a variation in  $v \sin i$  of  $\sim 25\%$  which we did not find.

No systematic variations were found in the equivalent widths of the H I or He I lines when binned on the 5.6 day orbital period. However, when binned as a function of the 294 day X-ray period of Priedhorsky, Terrell, and Holt (1982), there is an obvious maximum in the H $\gamma$  and H $\beta$  equivalent widths at X-ray phase 0 which corresponds to the time of minimum X-ray flux. The equivalent widths, normalized with respect to the mean value for each line, are listed in Table 8 and plotted as a function of the 294 X-ray phase in Figure 5. The estimated errors in the sixth column of Table 8 are based on a maximum error in equivalent width of 10% in each line and assume the error =  $10\%/N^{1/2}$ , where  $N$  is the number of spectra used in the determination of the equivalent width at each epoch.

The H $\alpha$  line is known (Ninkov, Walker, and Yang 1987) to be a composite of a P Cygni profile from the primary and weak emission from outflowing material. Other Balmer lines are also known to have small emission components (Gies and Bolton 1986). The observed change in H $\gamma$  and H $\beta$  equivalent widths might be due to variation in this emission component, but, if

TABLE 8  
He I AND BALMER LINE EQUIVALENT WIDTHS AS A  
FUNCTION OF THE 294 DAY X-RAY PERIOD

294 Day X-Ray Phase	He I $\lambda 4471$	He I $\lambda 4713$	H $\beta$	H $\gamma$	Error
Mean EW (mÅ) .....	645	273	1232	1745	...
Normalized with Respect to the Mean Values Above					
0.492 .....	0.97	0.94	1.04	0.98	$\pm 0.04$
0.314 .....	0.98	0.97	0.83	0.96	$\pm 0.07$
0.467 .....	1.04	1.07	1.05	1.00	$\pm 0.05$
0.620 .....	0.97	1.00	0.97	0.91	$\pm 0.04$
0.802 .....	0.98	0.98	0.94	0.89	$\pm 0.05$
0.724 .....	1.02	1.03	0.99	0.97	$\pm 0.05$
0.834 .....	1.01	1.03	1.01	0.99	$\pm 0.04$
0.252 .....	...	0.93	1.00	...	$\pm 0.04$
0.009 .....	1.02	1.04	1.17	1.22	$\pm 0.03$

so, the change at H $\beta$  was expected to be much greater than at H $\gamma$ , which is not what is observed. Since the X-ray flux originates from the accretion onto the secondary of the outflowing material from the primary, the decrease in X-ray flux could be associated with a reduced mass outflow from the primary. Any such reduction in mass outflow would also reduce the Balmer-line emission component and consequently increase the equivalent width of the Balmer absorption lines.

Priedhorsky, Terrell, and Holt (1983) have suggested that a precession in the system from either the compact object, the primary, or a tilted accretion disk could produce the observed 294 day X-ray period. Precession of the primary would produce variations in the  $v \sin i$  of HDE 226868. We see no such change to a level of  $\sim 5\%$  (see Table 7). Dolan *et al.* (1979) have suggested that the very large increases in X-ray flux (X-ray high states) seen sporadically (see Liang and Nolan 1984) could be explained by an occasional alignment of  $g$ -mode oscillations in the primary producing an enhanced mass loss and thus an increased accretion rate.

#### VII. ANALYSIS

It is widely believed that the components in a tidally linked binary move into circular, synchronized orbits after a suitable time. For the parameters appropriate to the Cyg X-1 system, Press, Wiita, and Smarr (1975) conclude that the circularization time is longer than the synchronization time. As the radial-velocity curve found for HDE 226868 implies a circular orbit, they would conclude that the orbit is already synchronous. Alternatively, Savonije and Papaloizou (1983) suggest that circularization could occur on a time scale as short as 100 yr if the system passes through a resonance between the orbit and stellar pulsation mode. Thus if the report of Li (1979) based on historic Chinese records is correct that the Cyg X-1 supernova occurred only 400 yr ago, it is possible that the orbit could be circularized but not synchronized.

If the assumption of synchronism is made, then the angular rotation velocity of the star is the same as its orbital angular velocity or

$$v \sin i / K = R_{\text{cm}} / R_*, \quad (2)$$

where  $v \sin i = 94.3 \pm 5 \text{ km s}^{-1}$ ,  $K = 75.0 \pm 1 \text{ km s}^{-1}$ ,  $R_{\text{cm}}$  = distance between star and system center of mass, and  $R_*$  = radius of star.

It is believed that the primary of Cyg X-1 almost fills its Roche lobe (Conti 1978; Gies and Bolton 1986). The expression for the Roche radius from Paczyński (1974) gives

$$R_* = F * R_{\text{sep}} * [0.38 + 0.2 \log (M_p / M_x)]$$

where  $F$  = Roche lobe filling factor,  $R_{\text{sep}}$  = system components separation,  $M_p$  = mass of primary, and  $M_x$  = mass of secondary which substituted into equation (2) gives

$$v \sin i / K = F * [(M_p + M_x) / M_x] * [0.38 + 0.2 \log (M_p / M_x)].$$

The filling factor can be constrained to have values  $F < 1$ , which avoids catastrophic Roche lobe overflow, and  $F > 0.75$  to produce the necessary light curve variations close to an eclipse limit for  $i$  (Gies and Bolton 1986). Substituting the observed values into this last equation and carrying all the uncertainties gives

$$1.5 \leq M_p / M_x \leq 2.3.$$

Underhill (1983) collated mass estimates for O stars and concludes that most have masses between 20 and  $40 M_\odot$ . The

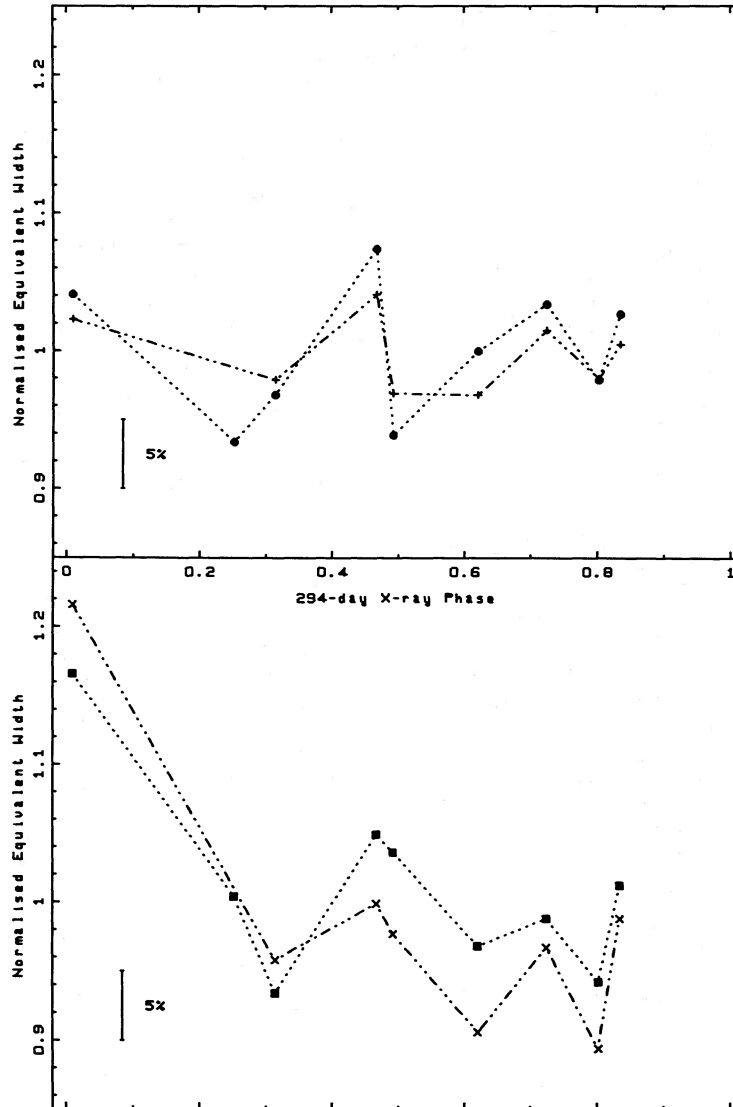


FIG. 5.—Upper box indicates He I  $\lambda 4471$  (dot-dash) and He I  $\lambda 4713$  (dotted) normalized equivalent widths at particular epochs of the 294 day X-ray period. Lower box is the same but for  $H\gamma$  (dot-dash) and  $H\beta$  (dotted). Mean error per plotted point is indicated.

typical mass of an O9.7 Iab is given by Schmidt-Kaler (1982) as  $25 M_{\odot}$ . Our estimate of the absolute magnitude of HDE 226868 from the  $H\gamma$  equivalent width is entirely consistent with its spectral type indicating a relatively normal O star. Assuming the minimum mass for the primary as the minimum observed for a normal O star (i.e.,  $20 M_{\odot}$ ) and using the above mass ratio gives a minimum mass for the secondary of  $9 \pm 1 M_{\odot}$  in agreement with the value found by Gies and Bolton (1986). This is much larger than the mass of neutron stars predicted by theoretical models ( $< 3 M_{\odot}$ ; Baym and Pethick 1979).

A study by Hutchings *et al.* (1979) found that the masses of primaries in X-ray binaries were less than their luminosities would imply. Rappaport and Joss (1983) have carefully examined the propagation of error in such mass determinations and find that although this effect is present, it is of the same order as the uncertainties.

Substituting our estimated range of the mass ratio, 1.5 to 2.3, and mass of the secondary into the mass function leads to a

system inclination of  $32^{\circ}$  to  $40^{\circ}$ . This is consistent with the UV line modeling estimate of  $36^{\circ} < i < 67^{\circ}$  (Davis and Hartmann 1983) and in the range  $25^{\circ} < i < 40^{\circ}$  as determined from X-ray polarization (Long, Chaman, and Novick 1980). Analyzing the optical light curve of this system, Gies and Bolton (1986) have determined an inclination of  $28^{\circ}$  to  $38^{\circ}$ , Guinan *et al.* (1979) have found  $43^{\circ}$  to  $53^{\circ}$  and Hutchings *et al.* (1973) found  $27^{\circ}$ .

It is not clear what significance to give the result from § V that the equivalent width of  $H\gamma$  is about 20% larger at phase zero on the 294 day X-ray period. It is not caused by a change in the continuum level since the equivalent widths of He I  $\lambda 4471$  and  $\lambda 4713$  lines are unchanged, but it could be due to an emission component in  $H\gamma$ . The Walker and Millward (1985) calibration gives an absolute magnitude of  $-6.3$  [ $W(H\gamma) = 1.8 \pm 0.1 \text{ \AA}$ ] and a distance of  $2.1 \pm 0.3 \text{ kpc}$  for the larger value of  $W(H\gamma)$  at zero X-ray phase. This smaller distance gives a lower range of minimum masses for the secondary (Paczynski 1974) of  $3.1$ – $4.8 M_{\odot}$ . As the reason for the changes in  $W(H\gamma)$  and  $W(H\beta)$  are unclear, these lower mass estimates

cannot be given much weight. We prefer the larger values for the distance and the mass of the secondary given in § V.

Z. Ninkov acknowledges the support of a Canadian Commonwealth Scholarship and Fellowship Plan Award and the facilities at the Department of Physics and Astronomy, Uni-

versity of Rochester where this paper was written. We are very grateful to Grant Hill and John Amor for their help in making the observations. P. Harmanec made useful comments on the manuscript, and we thank an anonymous referee for his helpful suggestions. This research was supported by funds to GAHW from the Natural Sciences and Engineering Research Council of Canada.

## REFERENCES

- Abt, H. A., Hintzen, P. A., and Levy, S. G. 1977, *Ap. J.*, **213**, 815.  
 Bahcall, J. N. 1980, in *Physics and Astrophysics of Neutron Stars and Black Holes*, ed. R. Giacconi and R. Ruffini (Amsterdam: North-Holland Press) p. 63.  
 Batten, A. H. 1973, *Binary and Multiple Systems of Stars*, (Elmsford, N.Y.: Pergamon Press).  
 Baym, G., and Pethick, C. 1979, *Ann. Rev. Astr. Ap.*, **17**, 415.  
 Beall, J. H., Knight, F. K., Smith, H. A., and Wood, K. S. 1984, *Ap. J.*, **284**, 745.  
 Bolton, C. T. 1972, *Nature*, **240**, 124.  
 ———. 1975, *Ap. J.*, **200**, 269.  
 Bowyer, S., Bryam, E., Chubb, T., and Friedman, H. 1965, *Science*, **147**, 394.  
 Bregman, J., Butler, D., Kemper, E., Koski, A., Kraft, R. P., and Stone, R. P. S. 1973, *Ap. J. (Letters)*, **185**, L117.  
 Brucato, R., and Kristian, J. 1973, *Ap. J. (Letters)*, **179**, L129.  
 Brucato, R. J., and Zappala, R. R. 1974, *Ap. J. (Letters)*, **187**, L71.  
 Conti, P. S. 1978, *Astr. Ap.*, **63**, 225.  
 Davis, R., and Hartmann, L. 1983, *Ap. J.*, **270**, 671.  
 Dearborn, D. S. P., and Eggleton, P. P. 1977, *Ap. J.*, **213**, 448.  
 Dolan, J. F., Crannell, C. J., Dennis, B. R., Frost, K. J., and Orwig, L. E. 1979, *Ap. J.*, **230**, 551.  
 Ebbets, D. 1979, *Ap. J.*, **227**, 510.  
 Gies, D. R., and Bolton, C. T. 1982, *Ap. J.*, **260**, 240.  
 ———. 1986, *Ap. J.*, **304**, 371.  
 Gray, D. F. 1976, *The Observations and Analysis of Stellar Photospheres* (New York: Wiley).  
 Guinan, E. F., Dorren, J. D., Siah, M. J., and Koch, R. H. 1979, *Ap. J.*, **229**, 296.  
 Herbig, G. H. 1975, *Ap. J.*, **196**, 129.  
 Herbison-Evans, D., and Lomb, N. R. 1971, *Comp. Phys. Comm.*, **3**, 368.  
 Hill, G., Walker, G. A. H., and Yang, S. 1986, *Pub. A.S.P.*, **98**, 1186.  
 Hutchings, J. B. 1976, *Ap. J.*, **203**, 438.  
 Hutchings, J. B., Cowley, A. P., Crampton, D., van Paradijs, J., and White, N. E. 1979, *Ap. J.*, **229**, 1079.  
 Hutchings, J. B., Crampton, D., Glaspey, J. W., and Walker, G. A. H. 1973, *Ap. J.*, **182**, 549.  
 Janes, K., and Adler, D. 1982, *Ap. J. Suppl.*, **49**, 425.  
 Kemp, J. C., Herman, L. C., and Barbour, M. S. 1978, *A.J.*, **83**, 962.  
 Kopylov, I. M., and Sokolov, V. V. 1984, *Soviet Astr. Letters*, **10**, 315.  
 Kundt, W. 1979, *Astr. Ap.*, **80**, L7.  
 Li, Q. B. 1979, *Chinese Astronomy*, **3**, 315.  
 Liang, E. P., and Nolan, P. L. 1984, *Space Sci. Rev.*, **38**, 353.  
 Long, K. S., Chaman, G. A., and Novick, R. 1980, *Ap. J.*, **238**, 710.  
 Lucy, L. B., and Sweeny, M. A. 1971, *A.J.*, **76**, 544.  
 Margon, B., Bowyer, S., and Stone, R. P. S. 1973, *Ap. J. (Letters)*, **185**, L113.  
 Mason, K. O., Hawkins, F. J., Sanford, P. W., Murdin, P., and Savage, A. 1974, *Ap. J. (Letters)*, **192**, L65.  
 Meinel, A. B., Aveni, A. F., and Stockton, M. W. 1975, *Catalog of Emission Lines in Astrophysical Objects* (Tucson: University of Arizona).  
 Moore, C. E. 1959, *A Multiplet Table of Astrophysical Interest, National Bureau of Standards Technical Note 36*, rev. ed.  
 Morbey, C. L. 1978, *Pub. Ap. Obs. Victoria*, **15**(4), 105.  
 Ninkov, Z., Walker, G. A. H., and Yang, S. 1987, *Ap. J.*, **320**, 438.  
 Ninkov, Z., Yang, S., Hill, G., and Walker, G. A. H. 1987, *Pub. A.S.P.*, in press.  
 Paczyński, B. 1974, *Astr. Ap.*, **34**, 161.  
 Press, W. H., Wiita, P. J., and Smarr, L. L. 1975, *Ap. J. (Letters)*, **202**, L135.  
 Priedhorsky, W., Terrell, J., and Holt, S. S. 1983, *Ap. J.*, **270**, 233.  
 Rappaport, S. A., and Joss, P. C. 1983, in *Accretion Driven Stellar X-Ray Sources*, ed. W. H. G. Lewin and E. P. J. van den Heuvel (Cambridge: Cambridge University Press), p. 24.  
 Savonije, G. J., and Papaloizou, J. C. B. 1983, *M.N.R.A.S.*, **203**, 581.  
 Schmidt-Kaler, Th. 1982, *The Stars*, in *Landolt-Bornstein, Numerical Data and Functional Relationships in Science and Technology*, New Series, ed. K. Schaifers and H. H. Vogt (Berlin: Springer-Verlag), Group VI, Volume 2, Subvolume b, p. 31.  
 Scholz, M. 1972, *Astr. Ap. Suppl.*, **7**, 469.  
 Seaton, M. J. 1979, *M.N.R.A.S.*, **187**, 73P.  
 Seyfert, C., and Popper, D. M. 1941, *Ap. J.*, **93**, 461.  
 Smith, H. E., Margon, B., and Conti, P. S. 1973, *Ap. J. (Letters)*, **179**, L125.  
 Sokolov, V. V., and Tsybal, V. V. 1984, *Soviet Astr. Letters*, **10**, 172.  
 Stoockley, T. R., and Mihalas, D. 1973, N.C.A.R. Technical Note STR-84.  
 Stumpff, P. 1979, *Astr. Ap.*, **78**, 229.  
 Underhill, A. B. 1983, *Hvar Observatory Bulletin*, **7**, 1.  
 Walborn, N. R. 1973, *Ap. J. (Letters)*, **179**, L123.  
 Walker, E. N., and Quintanilla, A. R. 1978, *M.N.R.A.S.*, **182**, 315.  
 Walker, G. A. H., Johnson, R., and Yang, S. 1985, in *Adv. Electronics Electron Phys.*, **64A**, 213.  
 Walker, G. A. H., and Millward, C. G. 1985, *Ap. J.*, **289**, 669.  
 Webster, B. L., and Murdin, P. 1972, *Nature*, **235**, 37.  
 Wilson, R. E., and Fox, R. K. 1981, *A.J.*, **86**, 1259.  
 Wu, C. C., Eaton, J. A., Holm, A. V., Milgrom, M., and Hammerschlag-Hensberge, G. 1982, *Pub. A.S.P.*, **94**, 149.

Z. NINKOV: Department of Physics and Astronomy, University of Rochester, Rochester, NY 14627

G. A. H. WALKER and S. YANG: Department of Geophysics and Astronomy, University of British Columbia, 2075 Westbrook Mall, Vancouver, B.C., V6T 1W5 Canada